

# ISTITUTO NAZIONALE DI FISICA NUCLEARE

Sezione di Genova

---

INFN/TC-98/17  
13 Luglio 1998

Ph. Bernard, G. Gemme, R. Parodi, E. Picasso:  
**COUPLED MICROWAVE CAVITIES FOR THE DETECTION OF SMALL  
HARMONIC DISPLACEMENTS**

**PACS: 07.57.K**

*Published by SIS-Pubblicazioni  
Laboratori Nazionali di Frascati*

## **COUPLED MICROWAVE CAVITIES FOR THE DETECTION OF SMALL HARMONIC DISPLACEMENTS**

Ph. Bernard <sup>1)</sup>, G. Gemme <sup>2)</sup>, R. Parodi <sup>2)</sup>, E. Picasso <sup>3)</sup>

<sup>1)</sup> CERN, CH-1211, Geneva 23, Switzerland

<sup>2)</sup> INFN-Sezione di Genova, Via Dodecaneso 33, I-16146 Genova, Italy

<sup>3)</sup> Scuola Normale Superiore, Piazza dei Cavalieri 7, I-56126, Pisa, Italy

### **Abstract**

The detection of weak forces acting on macroscopic bodies often entails the measurement of extremely small displacements of these bodies or their boundaries. This is the case in the attempts to detect gravitational waves or in the search for possible new long range interactions. In 1978 Bernard, Pegoraro, Picasso and Radicati suggested that superconducting coupled cavities could be used as a sensitive detector of gravitational effects, through the direct coupling of the gravitational wave with the electromagnetic field stored inside the cavities. In 1984 Reece, Reiner and Melissinos, built a detector of the type proposed in the 10 GHz frequency range, and used it as a transducer of harmonic mechanical motion. They achieved a sensitivity to fractional deformations of the order  $\delta x/x = 4 \cdot 10^{-18}$ . Our proposal is to repeat the Reece, Reiner and Melissinos experiment, increasing the detector sensitivity by a factor of  $10^3$ , thus reaching a sensitivity to fractional deformations of the order  $10^{-21}$ . If these results would be obtained this detector could be an interesting candidate for the detection of gravitational waves or in the search of long range interactions of weak intensity.

## 1. - INTRODUCTION

The detection of weak forces acting on macroscopic bodies often entails the measurement of extremely small displacements of these bodies or their boundaries. This is the case in the attempts to detect gravitational waves<sup>(1)</sup> (g.w.) or in the search for possible new long range interactions<sup>(2)</sup>.

In 1978 Bernard, Pegoraro, Picasso and Radicati suggested that rf superconducting coupled cavities could be used as a sensitive detector of gravitational effects<sup>(3)</sup>.

It has been shown that the principle that underlies this detector is analogous to the one used in parametric processes and in particular in frequency converters, i.e. in a device which converts energy from a reference frequency to a signal at a different frequency as a consequence of the time variation of a parameter of the system. An interesting aspect of the proposed detector is that it will respond to gravitational perturbations either through their direct coupling to the electromagnetic field, provided that a suitable geometric configuration of the detector is chosen (*direct* interaction of the gravitational wave with the electromagnetic fields enclosed inside the detector); or via the modification of the boundary conditions due to the interaction of the g.w. with the cavity walls (*indirect* interaction).

In more detail the rf superconducting coupled cavities detector consists of an electromagnetic resonator, with two level whose frequencies  $\omega_s$  and  $\omega_a$  are both much larger than the frequency  $\Omega$  of the g.w. and satisfy the resonance condition  $\omega_a - \omega_s = \Omega$ . In the scheme suggested by Bernard et al.<sup>(3)</sup> the two levels are obtained by coupling two identical high frequency resonators. The frequency  $\omega_s$  is the frequency of the level symmetrical in the fields of the two resonators, and  $\omega_a$  is that of the antisymmetrical one. The g.w. through its coupling to the electromagnetic energy can induce a transition between the two levels, provided their angular momenta along the direction  $z$  of propagation of the g.w. differ by 2. This can be achieved by putting the two resonators at right angle.

In the reference frame where the detector's walls are at rest, the energy transfer between the two levels can be entirely attributed to the time dependence of the anisotropic dielectric tensor  $\epsilon$  and of the magnetic permeability tensor  $\mu$  induced in vacuum by the g.w. as demonstrated in the first paper of ref. [3]. The power exchanged between the detector and the g.w. is in general proportional to the incoming gravitational flux, and to the electromagnetic energy  $U$  in the detector; it depends upon the mechanical properties of the detector ( $\Lambda$ ), the derivative of the correction to the metric tensor due to the g.w. in the transverse traceless gauge ( $\dot{a}$ ) and the

quadrupole moment associated with the configuration of the electromagnetic field ( $\Pi$ ). In formula the power exchanged is given by<sup>(3)</sup>:

$$P = \Lambda \text{tr}(\dot{a}\Pi)U \quad (1)$$

In the simplified case where the mechanical properties of the detector are described in terms of a single frequency  $\omega_m$  and a relaxation time  $1/(2\gamma_m)$ , the coefficient  $\Lambda$  takes the form:

$$\Lambda \approx \frac{\Omega^2}{\Omega^2 - \omega_m^2} \quad \text{for } |\Omega - \omega_m| > \gamma_m \quad (2)$$

and

$$\Lambda \approx \frac{\omega_m}{\gamma_m} = Q_m \quad \text{for } \Omega = \omega_m \quad (3)$$

In writing these relations we have neglected terms of order  $L^2\Omega^2$  where  $L$  is the characteristic size of the detector. As one can see from eq. (3) the case of rigid walls, where  $\omega_m \gg \Omega$ , leads to a strong reduction of the absorbed power. In the reference frame in which the walls are at rest the mechanical effect vanishes.

A parametric converter of the type proposed in ref. [3] has been built and used as an harmonic mechanical motion transducer in 1984 by Reece, Reiner and Melissinos (RRM)<sup>(4)</sup>. In order to measure the sensitivity limit of the detector, one of its walls was excited by an harmonic perturbation (by a piezoelectric); the results showed a sensitivity to relative deformations  $\delta x/x \approx 10^{-18}$ . Since in the RRM experiment the interest was to measure small harmonic displacements and *not* gravitational effects, they used two identical cylindrical cavities mounted *end-to-end* and coupled via a small circular aperture in their common endwall.

We wish to repeat the RRM experiment and improve its sensitivity by a factor  $10^3$ , thus reaching a sensitivity to harmonic displacements of the order  $10^{-21}$ . If these goal would be obtained this detector could be an interesting candidate for the detection of gravitational waves or in the search of long range interactions of weak intensity.

In the next section the physical principles of parametric power conversion are revised; in section 3 the sensitivity limits of the experimental apparatus are discussed. The mechanical and electromagnetic design of the detector is described in section 4, and in section 5 the preliminar tests performed on a detector model are shown. In the last section future developments of our project are briefly outlined.

## 2. – PHYSICAL PRINCIPLES OF PARAMETRIC POWER CONVERSION

A parametric converter (PACO) is a nonlinear device which transfers energy from a reference frequency to a signal with different frequency, utilizing a nonlinear parameter (a reactance) of the system, or a parameter that can be varied as a function of time by applying a suitable signal. The time varying parameter may be electrical or mechanical; in the latter case the device acts as a transducer of mechanical displacements.

The basic equations describing the parametric converter are the Manley-Rowe relations<sup>(5)</sup>. They are a set of power conservation relations that are extremely useful in evaluating the performance of a parametric device. We will not derive here the complete Manley-Rowe relations, but we will just describe the fundamental ideas upon which the parametric converter behavior is based.

Let us consider a physical system which can exist in two distinct energy levels. To fix our ideas let us take as an example a system of two identical coupled resonant cavities like those of the RRM experiment. If the resonant frequency of the unperturbed single cell is  $\omega_0$ , then the frequency spectrum of the coupled system consists of two levels at frequencies  $\omega_s$  and  $\omega_a$ , where  $\omega_s = \omega_0 - \delta\omega$  and  $\omega_a = \omega_0 + \delta\omega$ , where  $2\delta\omega/\omega_0 = K$ , is the coupling coefficient of the system.

We can store some electromagnetic energy in the system at frequency  $\omega_s$ ; if some external harmonic perturbation at frequency  $\Omega = \omega_a - \omega_s$  induces the time variation of one system parameter we can have some energy transfer between the two energy levels, i.e. from  $\omega_s$  to  $\omega_a$ . The external perturbation can equally well be an harmonic modulation of the cavity end wall, which causes the variation of the system reactance, or, in the case of the passage of a gravitational wave, the induced time modulation of the permittivity of the vacuum<sup>(6)</sup>.

Let us call  $P$  the total power absorbed by the device. We can write

$$P = P_s + P_a = \dot{N}_s \hbar \omega_s + \dot{N}_a \hbar \omega_a \quad (4)$$

where  $\dot{N}_i$  is the time variation of the number of photons in level  $i$ . If we assume that the total number of photons in the systems  $N = N_s + N_a$  is conserved we have

$$\dot{N}_a = -\dot{N}_s = \dot{N} \quad (5)$$

The total power absorbed by the system is therefore

$$P = \dot{N} \hbar (\omega_a - \omega_s) \quad (6)$$

and the power transferred to the upper level is given by

$$P_2 = \dot{N}\hbar\omega_a = \frac{P}{\hbar(\omega_a - \omega_s)} \hbar\omega_a = \frac{\omega_a}{\Omega} P \quad (7)$$

The amplification factor  $\omega_a/\Omega$  is characteristic of parametric frequency converters.

To get deeper insight into eq. (7) we have to know the exact expression of  $P$ ; in fact the power exchanged between the external perturbation and the system is proportional to the square of the fractional change of the time varying system parameter. If we denote this quantity with  $h$ , we can write for our coupled resonators system<sup>(4)</sup>:

$$P = \Omega U_s Q h^2 \quad (8)$$

We point out that the converted power does not depend on the mechanical properties of the device. This situation is somehow different from the general case discussed in the first paper of ref. [3], where the converted power *does* depend on the mechanical properties of the detector and is in fact maximum when the perturbing frequency  $\Omega$  equals the frequency of a mechanical resonance of the structure. The reason of this discrepancy is in the underlying physical process that takes place in either case. If we think of our device as a simple mechanical resonator we can describe its interaction with a g.w. as a forced oscillation at frequency  $\Omega$ . Obviously the amplitude of the oscillations will depend on  $\Omega$  and will be maximum for  $\Omega = \omega_m$ , where  $\omega_m$  is the frequency of a mechanical resonance of the structure. Since the converted power is proportional to the square of the wall displacement it will be maximum for  $\Omega = \omega_m$  as well. In our case (and also in the RRM experiment) we force the system with an harmonic perturbation at fixed amplitude determined by the voltage applied on the piezo; this fact drops out the dependence on mechanical properties in eq. (8).

From eq. (7) and eq. (8) we can easily derive the expression for the power transferred to the initially empty level

$$P_a = \omega_a U_s Q h^2 \quad (9)$$

In the last equation  $U_s$  is the energy stored in level  $s$ ,  $Q$  is the electromagnetic quality factor of the resonant cavities.

The quantity  $h$  above may represent the fractional change of the system reactance, or of the system length being harmonically modulated ( $\delta x/x$ ), or the dimensionless amplitude of the g.w.<sup>(6)</sup>

Since  $P_a$  is proportional to the electromagnetic quality factor, superconducting resonant cavities should be employed to achieve maximum sensitivity.

### 3. – SENSITIVITY LIMITS

Equation (9) could be a good starting point for a detailed discussion of the sensitivity limits of the detector. To make quantitative statements we need to know in some more detail our detector geometry. We choose a configuration very similar to the RRM experiment with two cylindrical niobium cavities coupled through a small circular aperture on the axis. The operating mode is the  $TE_{011}$  at 3 GHz which, due to the coupling, splits into a symmetrical and an antisymmetrical mode respectively at frequency  $\omega_s$  and  $\omega_a$ . The system is designed so that mode separation is about 1 MHz (see next section for more details on system design). For our geometry the relation between the maximum energy that can be stored in a superconducting niobium cavity and the frequency of the electromagnetic field is (in the following were not differently specified we take  $\omega_s \approx \omega_a = \omega$ )

$$\omega^3 U_{\max} \approx 8.9 \cdot 10^{31} \text{ Joule} \left( \frac{\text{rad}}{\text{sec}} \right)^3 \quad (10)$$

From eq. (10) we find at 3 GHz:

$$\omega U_{\max} = \frac{8.9 \cdot 10^{31}}{\omega^2} \approx 2.5 \cdot 10^{11} \text{ Joule} \frac{\text{rad}}{\text{sec}} \quad (11)$$

Deriving  $h$  from eq. (9) and using the above result we get:

$$h_{\min} \approx \left( \frac{P_a^{\min}}{Q \omega U_{\max}} \right)^{1/2} (\text{Hz})^{-1/2} \approx 10^{-16} \omega \left( \frac{P_a^{\min}}{Q} \right)^{1/2} (\text{Hz})^{-1/2} \quad (12)$$

where  $P_a^{\min}$  is the noise power spectral density in our system. From eq. (12) is apparent that to get better sensitivity lower frequencies and higher quality factors are preferred.

For example at 3 GHz with  $Q = 10^{10}$  and setting a noise power spectral density  $P_a^{\min} = 10^{-22}$  Watt/Hz we get  $h_{\min} \approx 2 \cdot 10^{-22} (\text{Hz})^{-1/2}$ ; while at 300 MHz, with  $Q = 10^{11}$  and the same noise power spectral density one should get  $h_{\min} \approx 6 \cdot 10^{-24} (\text{Hz})^{-1/2}$ .

To give a more realistic estimate of  $P_a^{\min}$  we have to discuss the various noise contributions present in our apparatus.

### 3.1. – Simmetrical mode leakage

To operate our device we have to feed microwave power into one resonant mode and then to perturb one system parameter at a frequency equal to the mode separation, in order to detect the energy transfer between the full and the empty mode. Here we suppose that the initially full mode is the symmetrical one, and that this same mode is the lower frequency one. This is very likely to be the case, but is not at all crucial for the following discussion.

To feed power into our device we shall use a voltage controlled microwave oscillator locked onto the cavity symmetrical mode, at frequency  $\omega_s$ . If we assume a lorentzian power distribution and a constant power of the lower (symmetrical) level we get:

$$P_{osc} \approx \frac{\frac{4P_0Q}{\omega_s}}{1+Q^2\left(\frac{\omega}{\omega_s}-\frac{\omega_s}{\omega}\right)^2} \frac{\text{Watt}}{\text{Hz}} \quad (13)$$

Here and in the following equations the suffix  $s$  labels quantities related to the symmetric mode, while the suffix  $a$  stands for the antisymmetric mode. From the above equation we can estimate the local oscillator noise power spectral density at the antysimmetric frequency, i.e. the leakage of mode  $s$  at the frequency of mode  $a$ :

$$P_a^{osc}(\omega_a) = \frac{\frac{4P_0Q}{\omega_s}}{1+Q^2\left(\frac{\omega_a}{\omega_s}-\frac{\omega_s}{\omega_a}\right)^2} \approx R \cdot \frac{U_s}{Q^2} \left(\frac{\omega_a}{\Omega}\right)^2 \frac{\text{Watt}}{\text{Hz}} \quad (14)$$

where we used the approximate relation  $P_0Q \approx \omega_s U_s$  and put  $\Omega = \omega_a - \omega_s$ .

$R$  is a number which depends upon the details of the measurement; if the receiver does not discriminate the parity of the field at frequency  $\omega_a$ ,  $R$  is of order one. Discrimination of the parity, as in the RRM experiment, would considerably reduce this value. RRM made use of a magic tee to excite the symmetric mode trough the  $\Sigma$  port, and to detect the antisymmetric mode trough the  $\Delta$  port (see fig. 1a). With careful adjustments they obtained 70 dB isolation between the  $\Sigma$  and  $\Delta$  ports of the magic tee ( $R \approx 10^{-7}$ ).

Additional noise suppression should be achieved by improving the mode discrimination and detecting  $P_a$  in pure transmission (see fig. 1b). With the use of two additional cavity couplings and another magic tee, the input and output signals could be optimally separated. The input couplings



would be balanced so as to null the excitation of the second cavity mode produced by phase noise in the input. The output couplings would likewise be balanced to null the transmission of the symmetrical mode. By this arrangement the 70 dB isolation given by a balanced magic tee is used twice. In fact numerical simulations performed on this system configuration gave  $R \approx 10^{-13}$  for the transmission detection scheme. With this calculated value of  $R$ , setting  $U_s = U_{\max}$  and  $Q = 10^{10}$  we get, at 3 GHz,  $P_a^{\text{osc}} \approx 10^{-19}$  Watt/Hz for  $\Omega = 1$  KHz. At  $\Omega = 1$  MHz, the contribution of the symmetrical mode width is negligible compared to the thermal noise spectral density:  $P^{\text{thermal}} \approx kT = 2.5 \cdot 10^{-23}$  Watt/Hz at  $T = 1.8$  K<sup>(7)</sup>.

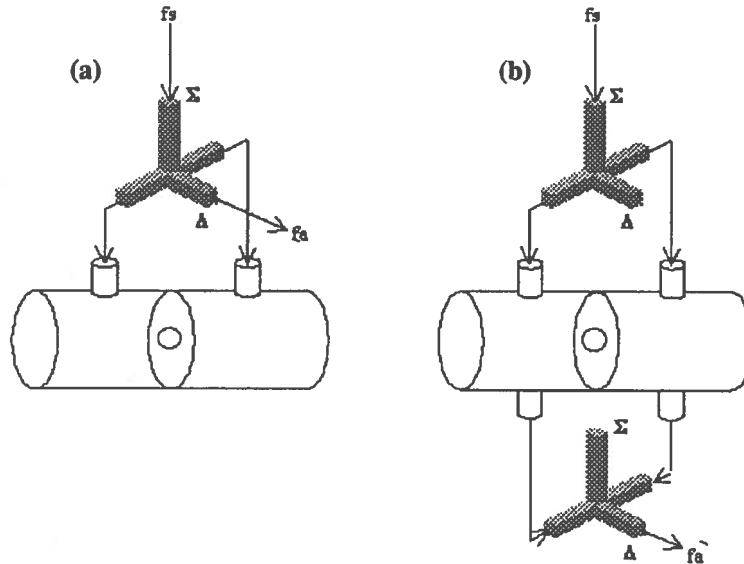


FIG. 1 - Schematic view of the experimental detection scheme (a) in reflection and (b) in transmission.

### 3.2. – Amplifier input noise

The input Johnson noise of the first amplifier in the detection electronics has to be evaluated and added to the former to establish the overall system intrinsic noise level.

The rf amplifier we are using is a JCA23-4029, manufactured by JCA Technology, Inc. which provides 48 dB gain at 3 GHz with a noise figure  $N_f = 0.6$  dB.

This leads to a thermal noise power spectral density at room temperature equal to

$$P_a^{\text{amp}} \approx kT \cdot 10^{N_f/10} = kT_{\text{eq}} \approx 5 \cdot 10^{-21} \text{ Watt/Hz} \quad (15)$$

We point out that this value is obtained at  $T = 300$  K which corresponds to  $T_{\text{eq}} \approx 340$  K. In principle using a cryogenic preamplifier one should gain more than an order of magnitude and get  $P_a^{\text{amp}} \approx 2.8 \cdot 10^{-22}$  Watt/Hz with an equivalent temperature  $T_{\text{eq}} = 20$  K.

### 3.3. – Brownian motion noise

Since we plan to operate our device as a mechanical motion transducer we must consider mechanical noise sources as well as electronic noise sources. In fact using eq. (9) we can write the brownian noise spectral density as

$$P_a^{\text{Br}} \approx \omega_a U_s Q (h^{\text{Br}})^2 \quad (16)$$

To derive an explicit expression of  $h^{\text{Br}}$  we have to develop a mechanical model of our system. Since it is quite difficult to treat the problem in the general case, and since we are interested in an order of magnitude estimate of the relevant quantities, we shall focus our attention on the longitudinal vibrational behaviour (i.e. on the mechanical displacements that change the cavity length) in two limiting cases:

- a) a low frequency limit  $\left( \omega_m \approx \frac{\pi c_s}{L} \right)$ , where the one-dimensional vibrational spectrum can be described by a discrete set of isolated resonances;
- b) an high frequency limit  $\left( \omega_m \gg \frac{\pi c_s}{L} \right)$ , where the system can be considered an elastic continuum.

#### 3.3.1. – Low frequency limit

The mean square displacement spectral density near a mechanical resonance is given by<sup>(8)</sup>

$$|x(\omega)|^2 = \frac{\frac{4kT\omega_m}{mQ_m}}{(\omega^2 - \omega_m^2)^2 + \left( \frac{\omega\omega_m}{Q_m} \right)^2} \frac{\text{m}^2}{\text{Hz}} \quad (17)$$

This amplitude is, from the parametric conversion process point of view, equivalent to the external perturbing signal. In other words we can associate to brownian motion a fractional change of the characteristic system length  $L$

$$h^{Br} \approx \frac{1}{L} \sqrt{|x(\omega)|^2} \approx \frac{1}{L} \left( \frac{\frac{4kT\omega_m}{mQ_m}}{(\omega^2 - \omega_m^2)^2 + \left(\frac{\omega\omega_m}{Q_m}\right)^2} \right)^{\frac{1}{2}} \frac{1}{\sqrt{\text{Hz}}} \quad (18)$$

Obviously the relevant contribution of brownian motion noise is for  $\omega \approx \Omega$ . We can slightly simplify the former expression in two limiting cases. When  $\Omega \approx \omega_m$  we have

$$(h^{Br})^2 \approx \frac{4kTQ_m}{mL^2} \frac{1}{\Omega^3} (\text{Hz})^{-1} \quad (19)$$

while if  $\Omega \gg \omega_m$  we have

$$(h^{Br})^2 \approx \frac{4kT}{mL^2} \frac{1}{Q_m} \frac{\omega_m}{\Omega^4} (\text{Hz})^{-1} \quad (20)$$

From eqs. (16), (19) and (20) we can write for the brownian noise power spectral density

$$P_a^{Br} \approx \frac{4kT}{mL^2} Q_m Q \frac{\omega_a}{\Omega^3} U \quad \text{For } \Omega \approx \omega_m \quad (21)$$

and

$$P_a^{Br} \approx \frac{4kT}{mL^2} \frac{Q}{Q_m} \frac{\omega_a \omega_m}{\Omega^4} U \quad \text{For } \Omega \gg \omega_m \quad (22)$$

To give a numerical estimate of this quantity the mechanical properties of the resonator should be known. If we set  $T = 1.8$  K,  $m = 10$  Kg,  $L = 1$  m,  $Q_m = 100$ ,  $Q = 10^{10}$  and  $U = U_{\max}$ , we get near a resonance for  $\Omega \approx \omega_m = 1$  KHz,  $P_a^{Br} \approx 10^{-11}$  Watt/Hz, which is largely the dominant contribution to the overall system noise.

From the above considerations is easily seen that to get an high sensitivity we should avoid to work at frequencies near to the detector mechanical resonances<sup>(9)</sup>.

### 3.3.2. – High frequency limit

Let us start our analysis by asking which is the mean vibrational energy per unit bandwidth in our system. We know that the mean energy per resonant mode is  $\varepsilon = kT$ , where we can safely neglect quantum-mechanical corrections for all frequencies of interest ( $\hbar\Omega \ll kT$ ). To find out the

mean energy per unit bandwidth we have to multiply the mean energy per mode by the number of modes per unit bandwidth at frequency  $\Omega$ :  $\sigma(\Omega)$ . It is well known that for a one-dimensional system this number does not depend on frequency and is equal to  $\sigma(\Omega) = \frac{L}{\pi c_s}$ , where  $c_s$  is the sound velocity in the solid considered. We have for the mean vibrational energy per unit bandwidth:

$$\left\langle \frac{dE}{d\Omega} \right\rangle = kT \frac{L}{\pi c_s} \quad (23)$$

If we compare the above expression with the energy of a one-dimensional harmonic oscillator at frequency  $\Omega$  we can write  $\langle dE \rangle = m\Omega^2 \langle x^2 \rangle d\Omega$ , where  $\langle x^2 \rangle$  is the mean square displacement spectral density and we can easily derive an expression for  $\langle x^2 \rangle$ :

$$\langle x^2 \rangle = \frac{kT}{m\Omega^2} \frac{L}{\pi c_s} \quad (24)$$

A this point is straightforward to find the expression that gives  $h^{Br}$  as a function of system parameters:

$$(h^{Br})^2 = \frac{\langle x^2 \rangle}{L^2} = \frac{1}{\pi c_s} \frac{kT}{m\Omega^2 L} \quad (25)$$

Using eq. (13) and setting  $T = 1.8$  K,  $m = 10$  Kg,  $L = 1$  m,  $c_s = 4.75 \cdot 10^3$  m/sec,  $Q = 10^{10}$  and  $U = U_{\max}$ , we get for  $\Omega = 1$  MHz,  $P_a^{Br} \approx 10^{-20}$  Watt/Hz, which is still the dominant contribution to the overall system noise.

### 3.4. – System sensitivity

All of the noise sources are incoherent. The total noise power spectral density is the sum of all the noise sources:  $P_a^{\min} = P_a^{osc} + P_a^{amp} + P_a^{Br}$ . Using the expressions found above we find the behaviour shown in fig. 2 of system sensitivity as a function of detection frequency. The values plotted in fig. 2 have been calculated for a signal to noise ratio of 1.7, corresponding to 90% confidence level for gaussian probability distribution. The peak at 1 kHz corresponds to a hypothetical mechanical resonance at that frequency. Due to the strong dependence of detector sensitivity to the mechanical properties of the device a detailed study of those properties is needed.

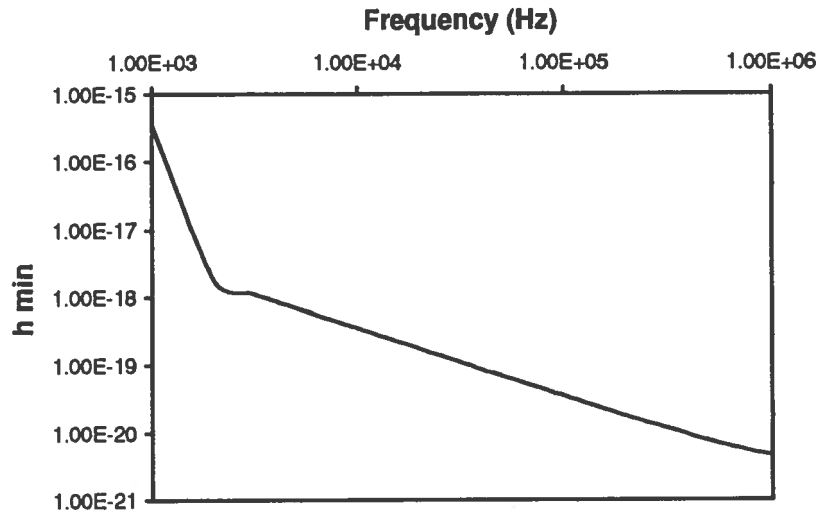


FIG. 2 - System sensitivity vs. detection frequency. Dominant noise contribution is thermal noise at all frequencies. Plotted values are for a signal to noise ratio of 1.7 (90% confidence level).

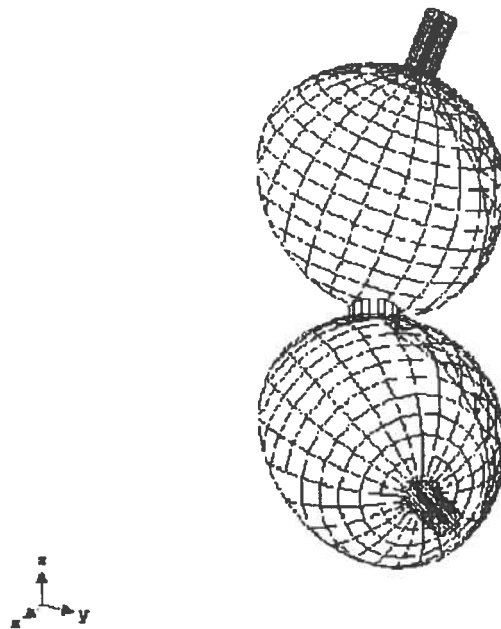


FIG. 3 - Schematic view of two coupled spherical cavities.

#### 4. – MECHANICAL AND ELECTROMAGNETIC DESIGN OF THE DETECTOR

The PACO detector is built using two coupled RF cavities. The geometry of the resonators gives us the electromagnetic field needed for the detection of the wanted physical quantities.

Because the ultimate sensitivity of the detector at a given frequency is related to the  $Q$  and the stored energy of the resonator, a resonator geometry with high geometric magnetic factor  $\Gamma$  is preferred, where

$$\Gamma = \omega_0 \mu_0 \frac{\int_V H^2 dV}{\int_S H^2 dS} \quad (26)$$

To avoid rf electronic vacuum discharges and Fowler-Nordheim like non resonant electron loading, rf modes with vanishing electric field at the surface are mandatory.

The aforementioned requirements on the field configuration in the coupled resonator force us to follow the same path of Reece, Reiner and Melissinos<sup>(4)</sup> choosing a TE mode for the cavities.

Early analysis of the best resonator shape suggested to use two spherical cavities coupled through an iris<sup>(10)</sup> as shown on figure 3; nonetheless the higher cost of this choice and the dimension of the spherical resonator suggested us to use as a first step a conservative and lower cost approach using two cylindrical cavities coupled through an axial iris (figure 4).

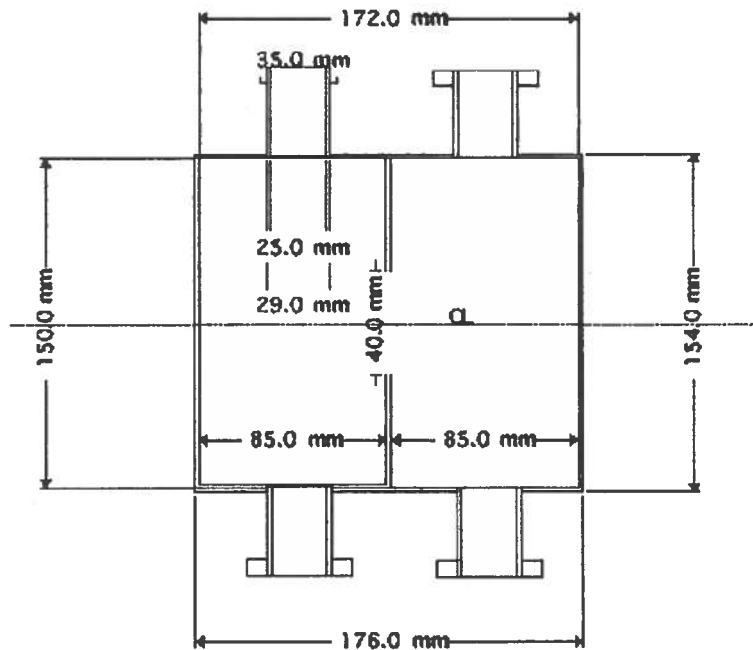


FIG. 4 - Schematic view of two coupled cylindrical cavities.

The choice of the frequency, at this stage, was imposed by the maximum dimension for the resonator that can be housed in our standard test cryostat in a comfortable way; in our case the inner diameter is 300 mm giving us enough room for a 3 GHz resonator.

The naive choice to start our design is a couple of cylindrical resonators having the height  $h$  equal to the diameter  $d$ .

For this configuration we can compute all the relevant quantities, as geometric factor and frequencies, starting from analytical expressions for the fields, or using the Bethe<sup>(11)</sup> perturbation theory for the evaluation of the coupling coefficient and mode separation.

Using a pill box like  $TE_{011}$  geometry nevertheless should be a little bit upsetting due to the degeneracy of the  $TE_{01}$  and  $TM_{11}$  modes; sure this problem is quite mild in our case: due to the very high  $Q$  value of the superconducting cavities, any distortion of the cavity geometry will split the TE and TM modes avoiding unwanted interactions.

Nevertheless we would like to enhance the splitting to be sure to remove any possible interaction between the TE and TM resonance.

To do that we design the cavity with a little modified geometry substituting the straight end plates with a spherical segment; the effect of this modification is to move away by 50 MHz the  $TM_{11}$  modes.

To compute the resonant frequency and the rf quantities relevant for our experiment we used our Oscar2D code<sup>(12)</sup>, the only code giving (in our knowledge) the geometric factors,  $Q$  and dissipation of TE cavities.

The selected geometry for the coupled resonators is reported on figure 5 with superimposed the magnetic field lines for the anti symmetric mode of the coupled resonators.

The relevant rf properties of the cavity modes are reported on Table I. Note that with the coupling hole diameter used in the calculation (40 mm) the mode splitting is about 1.9 MHz. At the final design stage the hole diameter will be  $\approx 35$  mm to have  $\Delta f \approx 1$  MHz.

The coupling iris is a circular hole on the cavity axis. The effect of the coupling gives a symmetric field distribution at the lower frequency and the anti symmetric at the higher frequency, i.e. the coupling is electrical.

Running the resonator geometry with different openings of the coupling hole we got informations about the sensitivity of the coupling on the iris diameter.

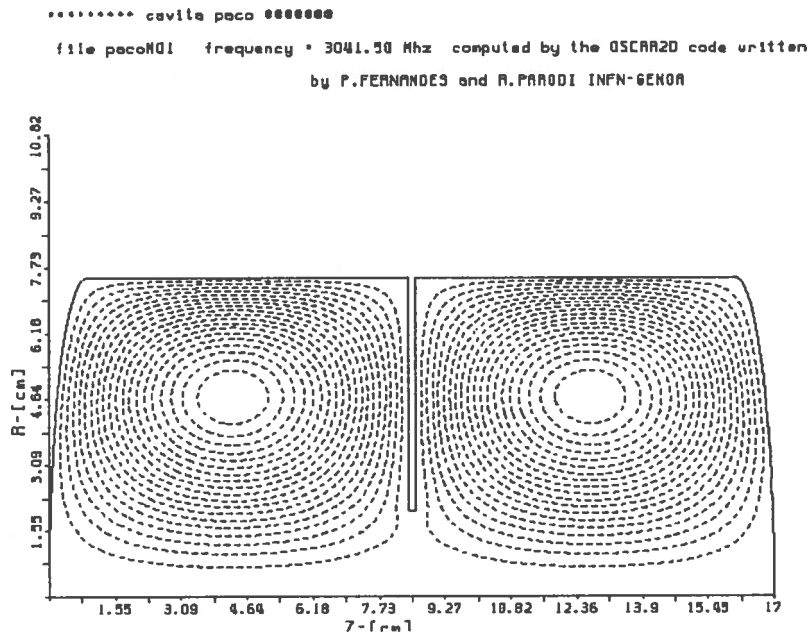


FIG. 5 - Plot of the anti-symmetric mode field lines superimposed on the longitudinal section of the resonator (only the upper half of the section is shown).

Last the effect of the coupling ports on the resonant frequency is evaluated computing the field distribution and scattering matrix for the full 3D problem (including the coupling loops) in a frequency interval centered on the operating frequency of the PACO detector. The full 3D simulations have been done with the Hfss<sup>TM</sup> package. The geometry of the 3D cavity model is shown on figure 6, the computed transmission coefficient  $S_{21}$  and reflection coefficient  $S_{11}$  on figure 7.

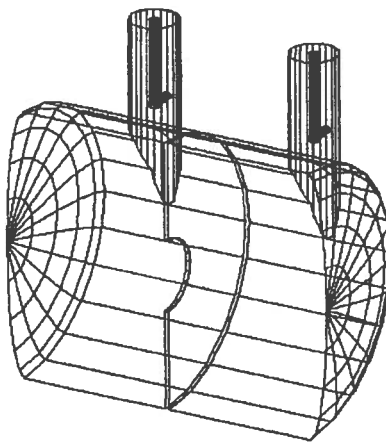


FIG. 6 - 3D model (longitudinal section) of the detector.



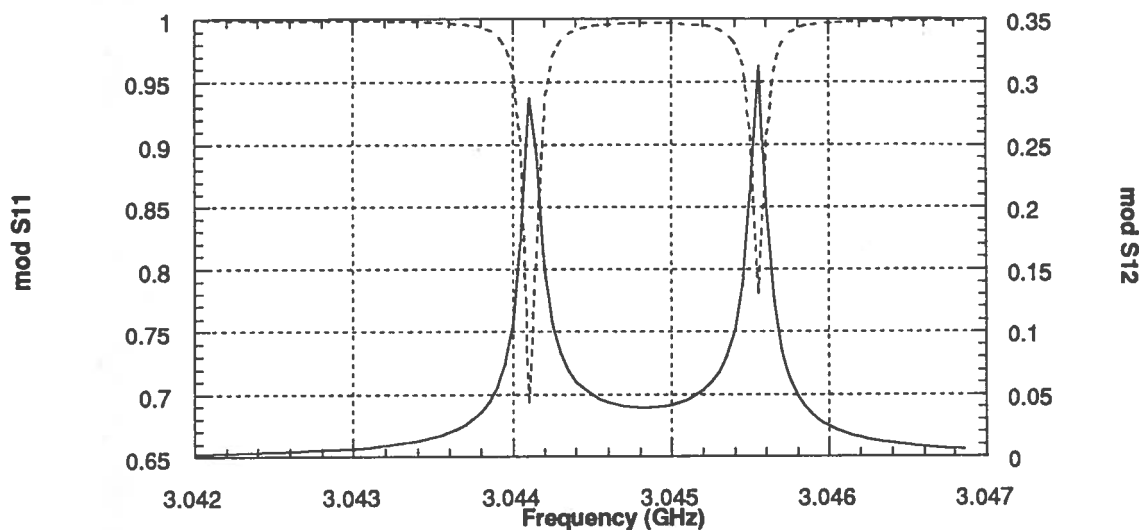


FIG. 7 - Computed transmission and reflection coefficients for the 3D structure.

The 3D simulation on the complete resonator confirmed the results of Oscar2D simulations either for the distribution of the resonant modes fields and the coupling coefficient for a given iris diameter.

On the basis of the results of the simulations the final design of the cavity was decided: the construction drawing of the PACO resonator is shown on figure 8.

## 5. – PRELIMINAR RESULTS

### 5.1. – Rf Tests on the PACO Model

To check our rf design for unforeseen flaws and bugs we built a normal conducting resonator model.

The barrel of the resonator was built using a standard brass tube, the end plates and the central septum using 5083 aluminium alloy.

This building technique allows us to change in a very fast way the coupling between the two cavities by changing the central septum.

Measured  $Q$  of the resonator was  $2 \cdot 10^4$  in good agreement with the computed one. In the Oscar2D runs we got  $Q$  values of  $2.4 \cdot 10^4$  using for the electrical resistivity of the brass  $8.8 \mu\Omega \cdot \text{cm}$  and  $5.5 \mu\Omega \cdot \text{cm}$  for the aluminium.

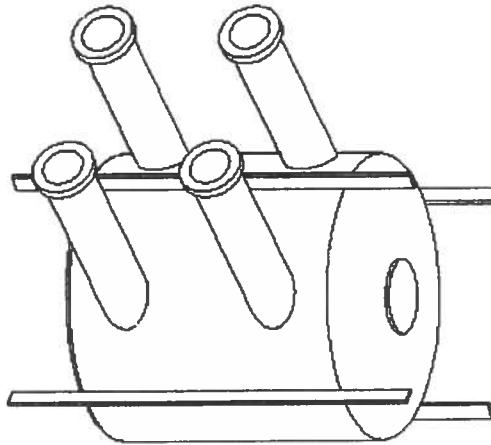


FIG. 8 - View of the final design of the PACO detector.

We also checked the mode distribution, driving the resonator either in a symmetric or in an antisymmetric way using two ports (having the same coupling coefficient), a coaxial magic tee, a phase shifter and two cables of the same electrical length.

The measurement showed the correctness of the computer simulation for the coupling giving the symmetric mode at the lower frequency and the antisymmetric one at the higher frequency of the  $TE_{01}$  band.

Figure 9 shows the transmitted power driving the system on the symmetric mode: the coupling iris is 40 mm in diameter.

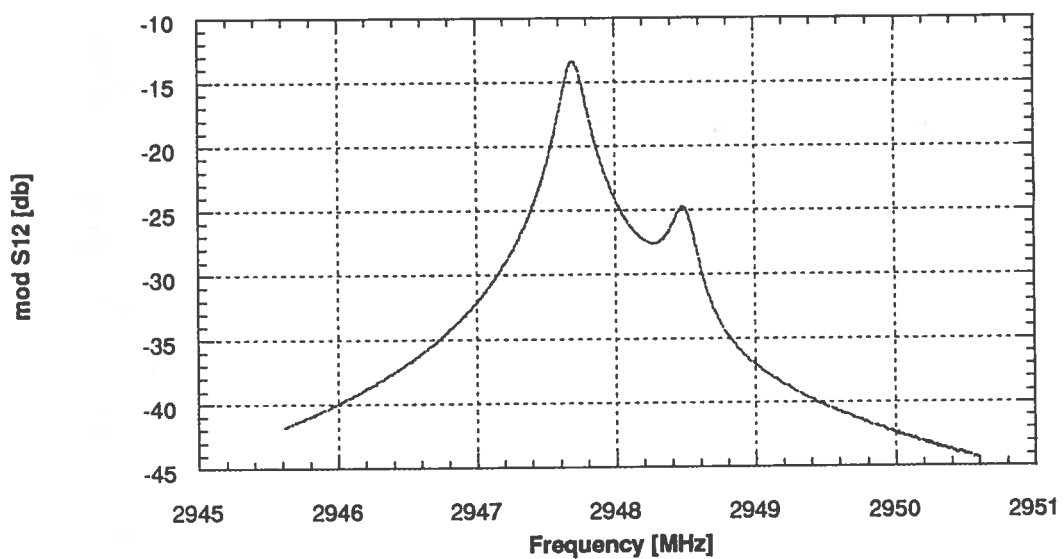


FIG. 9 - Transmitted power driving the system in the symmetric mode.

In the shown measurement we introduced a slight unbalance on the feed system of the cavity (a small phase offset) just to have a residual of the high frequency resonance as a reference.

The separation of the TE and TM modes was measured, for a 40 mm iris diameter the results are shown on figure 10.

Last we checked the accuracy of the computer simulations of the coupling of the resonators as a function of the iris diameter.

Due to the finite  $Q$  value of our resonator we should measure the mode splitting only for  $\Delta f$  greater than the resonator bandwidth (150 KHz).

The results of the simulations and of the measurements are shown on figure 11.

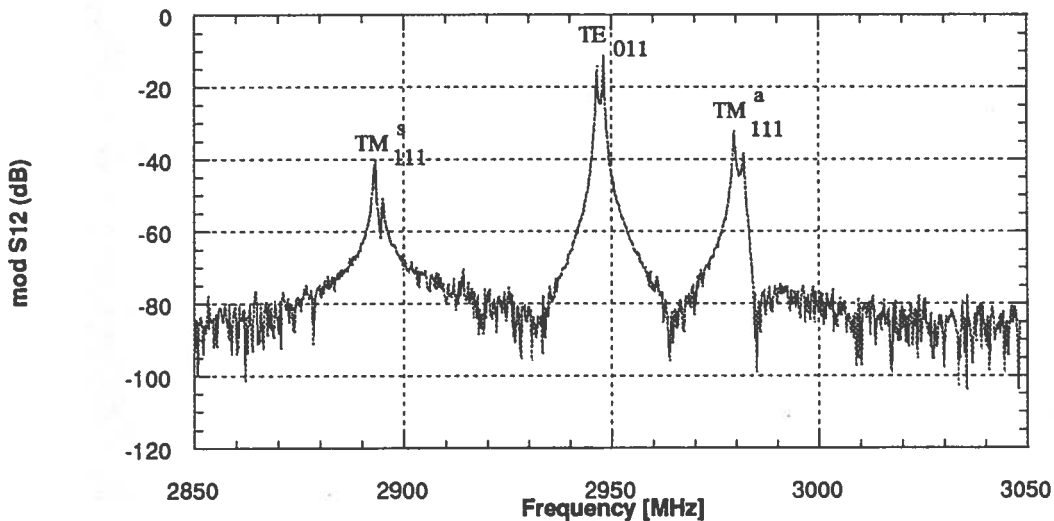


FIG. 10 - Mode separation for a 40 mm iris diameter.

The agreement (between the computed and measured values) is quite good on the whole range of iris diameters, the measured values are a little smaller than the computed one due iris wall thickness somewhat larger (2.1 mm) than the value used in the simulations (2 mm).

## 5.2. – Sensitivity Test of the PACO Model

The prototype resonator was also useful to check the behaviour of the whole system mainly to validate our simulations on the sensitivity of the parametric converter.

We set up the detector in both the “reflection mode“ set up and the “transmission mode“ setup, as shown on figure 1.

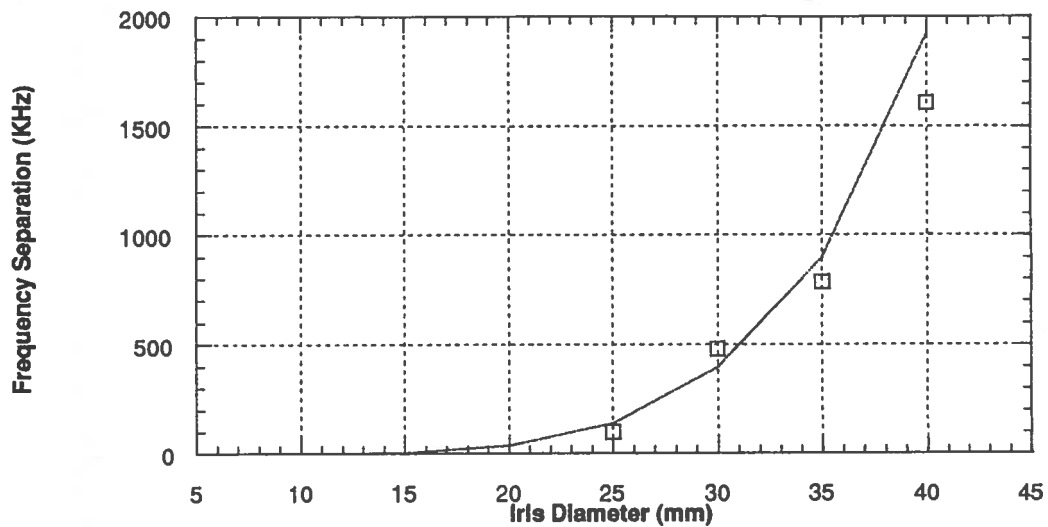


FIG. 11 - Computed and measured mode separation vs. iris diameter.

In that way we measured the improvement in sensitivity checking the obtained value of the symmetric mode component at the antisymmetric mode frequency.

In the case of the “reflection mode” we got a rejection value of  $R = -65$  dB by carefully tuning the phase and amplitude of the two feed lines. This is in good agreement with the value found by RRM with a similar experimental set-up.

In the transmission mode a rejection  $R = -100$  dB was obtained without pushing at the limit the optimization of the system: the experimental set up in fact allowed for an adjustment of the phase and the amplitude of the feed and detection lines; no optimization of the  $\Sigma$  and  $\Delta$  ports of the two coax magic tees was attempted.

The result of the experiment is reported on figure 12; the amplitude of the  $S_{12}$  coefficient as a function of the frequency offset from the antisymmetric mode nominal frequency is reported, showing a 100 dB rejection.

This result is quite encouraging and shows that the computed value of  $R = -130$  dB is a realistic estimate for an optimized system in the transmission configuration.

### 5.3. – Mechanical Analysis

Mechanical resonance of the resonator structure plays a quite important role in setting the ultimate sensitivity of the detector at a given mode as discussed in section 3.3.

Furthermore the knowledge of the deformation of the cavity walls (for a harmonic distortion of given amplitude and frequency) allows us to have a calibration of the detector when driven by a piezo-crystal in the test runs.

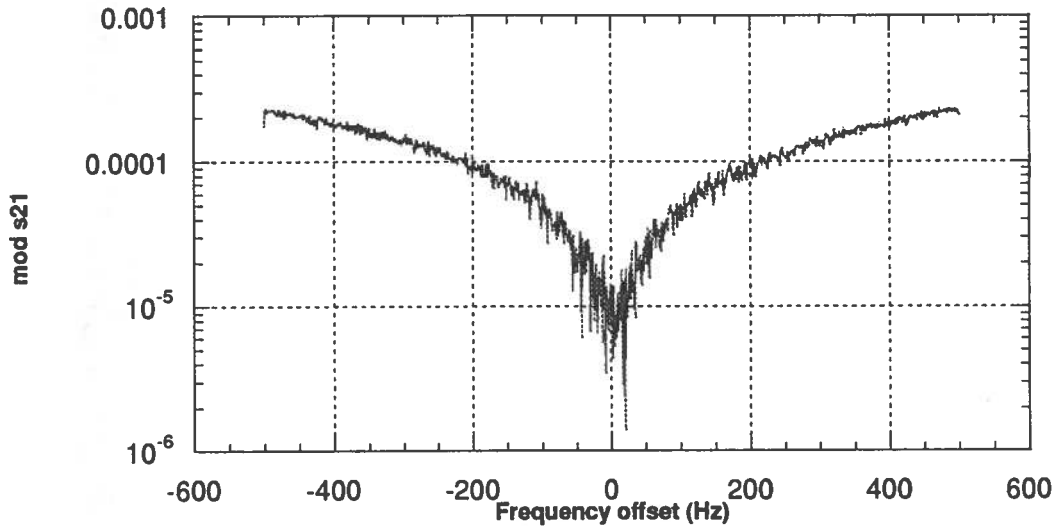


FIG. 12 - Symmetric mode transmission coefficient vs. frequency offset from the anti-symmetric mode frequency.

To estimate the modal spectra of the resonator and the response to a 1 mm displacement of a portion of the end wall we used the ANSYS™ mechanical analysis package.

The frequencies of the first 19 mechanical modes of the cavity, computed using a full 3D model are reported on Table II. The modes from 4 to 11 are all doubly degenerate. The shape of the first quadrupolar mode at the frequency of 1313.4 Hz is shown in figure 13.

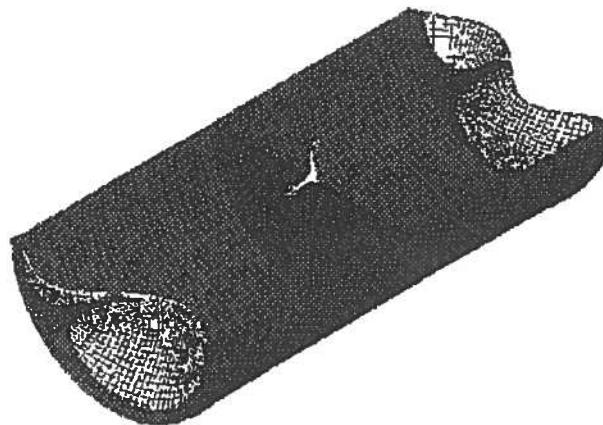


FIG. 13 - First quadrupolar mechanical mode of the structure at 1314.4 Hz.

After the modal analysis the study of the mechanical response to a fixed amplitude sinusoidal displacement of one end plate was performed using a 2D model to cope with the tiny mesh size needed at the higher frequencies to get meaningful results.

This simulations give us information about the corner frequency for the transition from the insulated mechanical resonances regime to the elastic continuum regime, giving again useful information about the influence of the thermal noise of the cavity walls on the detector ultimate sensitivity.

The harmonic analysis, performed at four frequencies 1 KHz, 10 KHz, 100 KHz and 1 MHz, showed a wall distortion decreasing with increasing frequency; the wall distortion for a drive frequency of 100 KHz and displacement amplitude of 1 mm is reported on figure 14.



FIG. 14 - Wall distortion for an harmonic drive frequency of 100 kHz (mag. 2000x).

## 6. - FUTURE PLANS AND CONCLUSIONS

Major efforts will be devoted in the near future to the development of the cryogenic system needed to test the superconducting detector. In the meantime the first version of the niobium cavity (cylindrical) is under construction. We plan to perform the first cryogenic test of the system in fall 1998 and to accomplish the final system set-up in early 1999.

Next year will be dedicated to establish system sensitivity by carefully studying the optimum detection parameters and understanding noise sources.

We shall concentrate our attention to the following main items:

TABLE I – Mechanical resonances spectrum of the detector.

Mode number	Frequency (Hz)
1	633.15
2	654.48
3	713.96
4a – 4b	1313.4
5a – 5b	1318.5
6a – 6b	1412.2
7a - 7b	1606.6
8a – 8b	1808.4
9a – 9b	1826.0
10a – 10b	1950.9
11a – 11b	2018.2

- System stability over time ranges of the order of magnitude of the inverse of our detection bandwidth. Obviously if we are going to detect our signal in a 10 mHz bandwidth, we have to check carefully that system parameters do not change significantly over a 100 sec time scale; in particular the most critical parameter is the frequency splitting between the two normal modes  $\Omega$ . Experimental tests will show if an active control is needed to lock  $\Omega$  at a fixed value.
- System sensitivity, by measuring noise level without any perturbing external signal. A careful analysis and comparison between theoretical predictions and experimental results on noise level will be done.
- Verification of parametric conversion, measuring the converted signal at different external perturbation amplitudes. This point includes optimum system tuning to get best signal to noise ratio.
- Mechanical modes distribution and properties measurement.

At the end of the experimental tests on the cylindrical detector, during 1999 we shall build and test the spherical cavities detector configuration, which should give best performances in view of gravitational waves detection, due to the more favourable electromagnetic geometric factor.

If the goal sensitivity would be obtained, the proposed detector could be an interesting candidate in the search of gravitational waves or long range interactions of weak intensity. In fact

it is conceivable to push down the rf operating frequency in the 300 MHz range and the mode splitting in the 10 kHz range, thus making a series of similar detectors, working at different frequencies and/or mode separations, covering the  $10^4 - 10^6$  Hz range. This frequency range is beyond the resonant bar and large bandwidth interferometers operating frequency so that the proposed detector could be useful to cover the high frequency region of the spectrum.

Recent works<sup>(13)</sup> focused their attention on the detection of stochastic g.w. sources and in particular of the relic g.w. background and pointed out that a relic background detected at high frequency would be unambiguously of cosmological origin. The detection of stochastic g.w. sources could be done by correlating two (or more) detectors put at a distance small compared to the g.w. wavelength (so that the signals could be correlated) but large enough to be sufficient to decorrelate local noises. With this experimental arrangement system sensitivity could be increased by several orders of magnitude<sup>(14)</sup> making possible the detection of very low signal levels.

## ACKNOWLEDGMENS

We wish to thank Dr. S. Farinon of INFN Genova for the valuable contribution given in the development and analysis of the detector mechanical model.



## REFERENCES

- (1) J. Weber, Phys. Rev. 117 (1960), 306; Nature 240 (1972), 28; Phys. Rev. Lett. 31 (1973), 779.
- (2) G. Feinberg and J. Sucher, Phys. Rev. D20 (1979), 1717; J.E. Moody and F. Wilczek, Phys. Rev. D30 (1984), 130.
- (3) F. Pegoraro, E. Picasso and L.A. Radicati, J. Phys 11A (1978), 1949; F. Pegoraro, L.A. Radicati, Ph. Bernard and E. Picasso, Phys. Lett. 68A (1978), 165.
- (4) C.E. Reece, P.J. Reiner and A.C. Melissinos, Phys. Lett. 104A, (1984), 341; Nucl. Instr. Meth. A245 (1986), 299.
- (5) J.M. Manley and H.E. Rowe, Proc. IRE, 44, (1956), 904; Proc. IRE, 47, (1959), 2115.
- (6) We remind that in order to couple with a g.w. the angular momenta along the direction of the g.w. of the two energy levels should differ by two. This can be achieved by putting the resonators at right angles. Obviously this is not the case neither in the RRM nor in our experiment. Nevertheless the statements made about parametric power conversion and system sensitivity are still valid provided that the perturbation amplitude ( $h$  in the following) is correctly interpreted.
- (7) We point out that even if in eq.(11)  $P_a^{osc} \rightarrow 0$  for  $\Omega \rightarrow \infty$ , this is not true because each resonant mode carries a thermal noise power spectral density  $P^{thermal} \approx KT$ .
- (8) P.F. Michelson, Phys. Rev. D, 34, (1986), (10).
- (9) We remark that this comment should be carefully discussed if the device has to be used as a g.w. detector, because as pointed out in section 2 and in ref. [3] in that case also the signal increases in correspondence with the mechanical resonances of the structure.
- (10) Ph. Bernard, G. Gemme, R. Parodi and E. Picasso, Eighth Workshop on Rf Superconductivity, Abano Terme, (1997).
- (11) H.A. Bethe, M.I.T. Radiation Laboratory Report, V-15S, (1942); 43-22, (1943); 43-26, (1943), 43-27, (1943); 43-30, (1943).
- (12) P. Fernandes and R. Parodi, IEEE Trans. Mag., 24, (1988), 154.
- (13) R. Brustein, M. Gasperini, M. Giovannini and G. Veneziano, Phys. Lett. B361, (1995), 45; B. Allen, gr-qc/960433, (1996); B. Allen and J. Romano, gr-qc/9710117, (1997).
- (14) M. Maggiore, gr-qc/9803028, (1998).